Interaction between femtosecond laser pulses and CdS_xSe_{1-x} quantum dots in glasses

R. Osellame,* R. Martinez Vazquez, G. Cerullo, R. Ramponi, and O. Svelto
Istituto di Fotonica e Nanotecnologie-CNR and Dipartimento di Fisica, Politecnico di Milano, Piazza L. da Vinci 32, I-20133 Milano, Italy

V. Russo, A. Li Bassi, and C. E. Bottani
Center for NanoEngineered MAterials and Surfaces (NEMAS), CNISM, and Dipartimento di Ingegneria Nucleare, Politecnico di Milano, Via Ponzio 34/3, I-20133 Milano, Italy

C. Spinella
Istituto per la Microelettronica e Microsistemi-CNR, Stradale Primosole 50, I-95121 Catania, Italy
(Received 22 December 2006; revised manuscript received 28 March 2007; published 31 July 2007)

Interaction between femtosecond laser pulses and semiconductor nanocrystals is thoroughly studied. Absorption, Raman, and photoluminescence spectra together with transmission electron microscopy images are presented for irradiated regions and compared to those of the pristine material. A simple model based on charge transfer to the glass matrix from the nanocrystals is adopted to explain the strong color changes and the photoluminescence quenching induced by the femtosecond laser pulses.

DOI: 10.1103/PhysRevB.76.045340 PACS number(s): 78.67.−n, 81.07.Ta, 33.80.Rv

I. INTRODUCTION

Semiconductor quantum dots embedded in glasses have been intensively investigated both as a basic research model for three-dimensional quantum confinement and for their very interesting optical properties.[1] Sharp edge absorption spectra, saturable absorption, and large nonlinear properties make these materials very useful for applications as sharp-cutoff filters,[2] Q-switching elements in lasers,[3] and all-optical switches for signal processing.[4]

Optical properties of nanostructured glasses strongly depend on the fabrication procedure that determines dot composition, size, and shape. A powerful postprocessing instrument to locally tailor the optical properties of such glasses is irradiation with a pulsed laser beam.[5]

Femtosecond laser systems are becoming more and more important in micromachining materials due to several reasons. The high peak intensity of the near-infrared ultrashort pulses allows nonlinear absorption at the focus of the laser beam even in transparent materials.[6] This, together with the low thermal diffusion, gives the possibility to deposit energy in a very localized volume anywhere inside the sample, thus creating a local modification of its optical properties. Moreover, the reliability, compactness, and ease of use of femtosecond laser systems are rapidly improving,[7] allowing one to envisage their use in an industrial environment.

In particular, femtosecond laser pulses have been widely used to induce permanent microscopic structural modifications in glasses containing metal nanoparticles.[8–11] In that case, the initial shape of the nanoparticles is modified, causing color changes and dichroism due to a shift in the surface plasmon resonances. On the other hand, the interaction of femtosecond laser pulses with semiconductor quantum dots has been studied only in a low-intensity perturbative regime for ultrafast dynamics investigations,[12] while no studies have concerned the possibility to induce permanent changes.

In this paper, we present a thorough study of the interaction of femtosecond laser pulses with CdS_xSe_{1-x} quantum dots embedded in a glass matrix. Permanent color changes have been obtained in the irradiated zones. Analyses with absorption and photoluminescence spectra, Raman scattering, and transmission electron microscopy have been performed in order to understand the origin of the modifications that the ultrashort pulses induce on the semiconductor quantum dots. A strong and permanent quenching of the quantum dots photoluminescence, induced by the femtosecond laser pulses, is observed.

II. EXPERIMENT

The investigated samples are commercially available long-pass filters from Schott Glass, Inc., which consist of CdS_xSe_{1-x} nanocrystals embedded in a borosilicate glass matrix. The volume fraction of the nanocrystals in the matrix is $\sim 1\%$. The optical properties of such filters are determined by the characteristics of the semiconductor nanocrystals embedded in the matrix. The nanocrystal diameter and its chemical composition are the most important parameters which determine the spectral position of the absorption edge and therefore the color and the cutoff wavelength of the glass filter. In this work, two different filters, with commercial names GG495 (pale yellow color) and OG530 (orange color), are studied.

These filters have been irradiated with a commercial regeneratively amplified Ti:sapphire laser (Legend, Coherent Inc.) that generates 40 fs pulses at 1 kHz repetition rate at a wavelength of 780 nm. The laser was focused on the substrates by a 50 cm focal length lens that permits achieving a maximum peak intensity of $\sim 2.2 \times 10^{14}$ W/cm^2. It is worth noting that despite the high peak intensity, the very short pulse duration and the low laser repetition rate avoid the occurrence of any thermal effect;[13] thus, we expect a material modification strictly related to the nonlinear absorption

mechanism. The samples were mounted onto a two-axis motorized stage (Physik Instrumente) for translation during irradiation. Translation occurred transversally to the writing beam at a speed of 200 μm/s, constant in all experiments. To obtain modified areas with larger dimensions, several linear scans were laterally juxtaposed. Due to the long confocal parameter of the femtosecond laser beam, the 2-mm-thick glass sample was uniformly modified in depth.

In order to investigate the variation in the absorption spectra, measurements in and out of the modified zones were performed using a JASCO V-570 spectrophotometer. The spectra were obtained at room temperature with a wavelength resolution of 0.5 nm and a scanning rate of 100 nm/min.

Raman spectroscopy was used as a fast and nondestructive technique to determine both the composition parameter x and the size of the nanocrystals.[14] The determination of x is based on the composition-dependent spectral positions and weights of the CdS-like and CdSe-like LO phonon peaks. The average size of the nanocrystals could be deduced from low-wave-number (LW) Raman bands which correspond to nanocrystal acoustic vibrations having size-dependent Raman shifts. In order to achieve a more direct analysis of the nanocrystal dimensions, bright-field transmission electron microscopy (TEM) in a cross-sectional configuration has been performed. The Raman experiments were performed with a Renishaw in Via Raman microscope with an argon ion laser excitation wavelength of 457 nm. The LW Raman spectra were collected using an excitation wavelength of doubled Nd-doped yttrium aluminium garnet laser at 532 nm and a T64000 Jobin-Yvon system with the triple grating configuration that allows low frequencies to be investigated. The photoluminescence (PL) measurements were performed by exciting the nanoparticles with an argon ion laser either at 457 nm or at 488 nm and collecting the signal in an orthogonal scattering geometry. The PL spectra were then acquired by an Ocean Optics high resolution spectrometer HR2000+. The TEM measurements were performed by using a JEOL JEM 2010 F microscope operating at an acceleration voltage of 200 kV.

The two kinds of Raman spectra, the PL spectra, and the TEM images were acquired in and out of the modified regions to investigate the influence of the femtosecond irradiation on the nanocrystals embedded in the samples.

III. RESULTS AND DISCUSSION

During femtosecond laser irradiation of the glass sample, a white light emission is clearly visible. This emission comes from the electron plasma generated by the nonlinear absorption of the femtosecond laser pulses, and is a useful indication that the incident intensity is above the modification threshold. After irradiation, the modified zones show a darker color which is permanent at room temperature. In Fig. 1, both glass filters are presented with modified and unmodified regions. It is worth noting that the same irradiation parameters induce much stronger color variations on the OG530 filter than on the GG495.

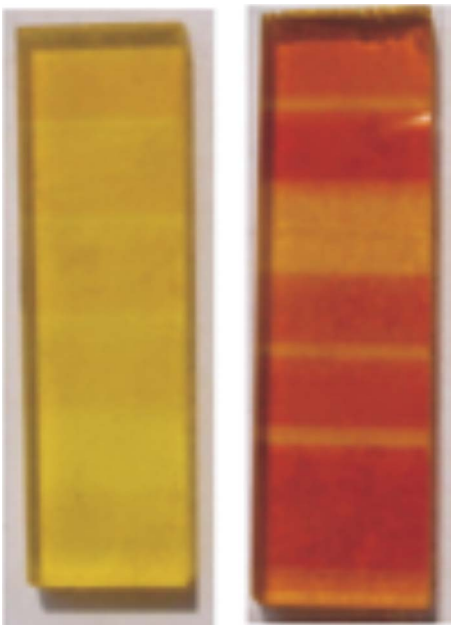

FIG. 1. (Color online) Pictures of the glass filters: (a) GG495 and (b) OG530. Darker regions are irradiated with the femtosecond laser.

A. Raman spectra

The color of the nanostructured glasses is strongly dependent on the dimension and composition of the embedded CdS_xSe_{1-x} nanocrystals. In fact, by varying these two parameters in the fabrication process, different cutoff filters are obtained covering the whole visible range. The evident color change shown in Fig. 1 could then be ascribed to a variation in either the size or the composition of the nanocrystals induced by the femtosecond laser pulses. In order to investigate this possibility, Raman measurements have been performed on the OG530 and GG495 samples in and out of the irradiated zones. The spectra, collected in the Stokes region, also show PL excited by the laser used for Raman investigation. In this kind of glasses, PL emission comes both from direct recombination at the absorption edge (usually not visible in Raman spectra due to filtering of the elastic scattering) and from deep traps lying below the edge (redshifted emission).[15] Since PL signal is often much stronger than the Raman one, it could be difficult to distinguish the latter. However, exploiting the resonance effect with a suitable laser wavelength, the Raman signal can be significantly enhanced (resonant Raman scattering). Raman spectra for the OG530 sample, performed with a 457 nm wavelength laser, are shown in Fig. 2(a). Raman signals from the unmodified and irradiated regions are clearly visible, thanks to the resonance effect (excitation at 2.7 eV with respect to the 2.3 eV band gap). The two bands at 198 cm^{-1} (LO_1) and 288 cm^{-1} (LO_2) are attributed to the LO phonons of CdSe- and CdS-like modes, respectively, in the composite CdS_xSe_{1-x} system.[16,17] The positions and relative intensity of these bands can be used to determine the composition of CdS_xSe_{1-x} nanocrystals embedded in the glass.[16] In the case

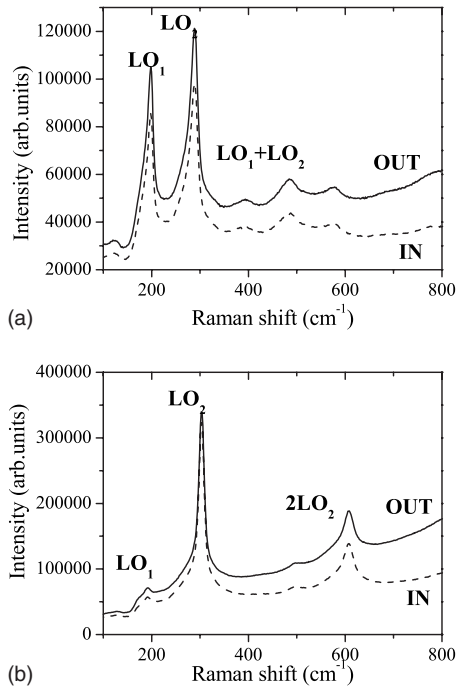

FIG. 2. (a) OG530 and (b) GG495 samples. 457 nm Raman spectra of the unmodified region (OUT) and of the region irradiated with 1.3×10^{14} W cm^{-1} femtosecond laser peak intensity (IN). The CdSe-like (LO_1) and CdS-like (LO_2) modes are indicated, together with the LO_1+LO_2 and $2LO_2$ second order Raman scattering contributions. No composition variation appears to be induced by the femtosecond laser pulses (see text).

of the OG530 filter, the spectrum in Fig. 2 suggests a similar content of selenium and sulfur in agreement with the values reported in the literature for this glass.[14] Also, the presence of a feature at about 490 cm^{-1}, attributed to LO_1+LO_2 second order Raman scattering and strong only for samples with comparable content of S and Se, would confirm this kind of composition.[18] In Fig. 2(b), Raman spectra in the two regions of the GG495 sample are reported, again performed with the 457 nm wavelength laser to exploit the resonance effect (2.7 eV compared to a band gap of 2.5 eV). In this case, the spectrum is characterized by a very strong band at 304 cm^{-1}, corresponding to LO_2 mode, that is, the CdS-like mode, and a weaker LO_1 contribution at 193 cm^{-1}. Accordingly, the second order spectrum presents a strong band at about 600 cm^{-1}, corresponding to $2LO_2$ Raman scattering, while the LO_1+LO_2 contribution becomes weaker. These features would confirm a greater content of sulfur in the GG495 filter, as reported in the literature.[14]

The aim of the Raman measurements, however, was to compare the results in and out of the modified region in order to understand if the femtosecond laser pulses had induced any variation in the nanocrystal composition. As evidenced in Fig. 2, no difference within the instrument resolution ($\sim$3 cm^{-1}) can be observed between the Raman spectra of the two regions for both filters. Therefore, we conclude that no composition variation is induced by femtosecond laser irradiation. For both samples, there is a reduction of the background intensity in the spectrum of the irradiated region with respect to the unmodified one. This feature is related to a decrease in the sample photoluminescence (see Sec. III B).

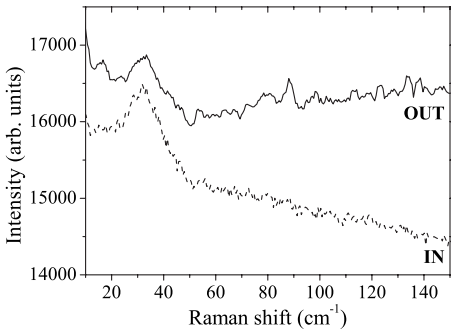

FIG. 3. Low frequency 532 nm resonant Raman spectra of OG530 sample. Comparison between unmodified (OUT) and modified (IN) regions. Similar position and shape of the symmetric acoustic mode in the two regions indicate that no size variation is induced by the femtosecond laser pulses (see text).

LW Raman spectra (>10 cm^{-1}) of the OG530 filter are reported in Fig. 3 for the modified and the unmodified regions. No polarization analysis was performed, even if a vertical-vertical polarization geometry would give a better signal-to-noise ratio for the observed mode[19] (see below). Anyway, the resonance effect seems to compensate for the lack of polarization analysis, allowing us to achieve a good signal in both regions. The low frequency Raman features correspond to the acoustic vibrations of the nanoparticles, and have been extensively studied assuming homogeneous, elastic, spherically shaped particles.[19,20] In particular, only two spheroidal modes are Raman active,[20] namely, the symmetric, purely radial, polarized mode (labeled by $l=0$ from the indices of the harmonic function Y_{lm}) and the quadrupolar unpolarized one ($l=2$). The frequencies of these modes are inversely proportional to the particle diameter.[14,21] However, the accurate determination of particle dimensions from the frequency of these modes is not so straightforward and it requires the knowledge of the longitudinal (for $l=0$) and transverse ($l=2$) velocities of sound in the CdS_xSe_{1-x} crystallites, usually interpolated from the corresponding velocities of bulk CdS and CdSe.[14] Comparing our results with data reported in the literature,[19,22] we can conclude that the band at about 30 cm^{-1} found in the spectrum of the OG530 filter corresponds to the symmetric mode ($l=0$). From the position of this mode, however, different models lead to different mean radii for the OG530 nanoparticles. For example, Ivanda *et al.*[19] give a value of about 3.9 nm, while Verma *et al.*[22] of about 2.2 nm, both from a Raman shift of about 30 cm^{-1}. As in the above discussion on nanocrystal composition, also in this case the goal of the measurement is not the absolute value of the radius but the comparison of the position and the shape of the LW bands in the spectra collected from the modified and unmodified regions of the OG530 sample, which appear very similar. It can be concluded that irradiation with femtosecond pulses does not vary appreciably the particle size distribution. For the GG495 filter, the LW Raman spectra do not provide significant information due to the lack in our T64000 JY system of a laser source with a wavelength suitable to exploit resonance ($\lambda < 495$ nm) and the absence of polarization geometry. There-

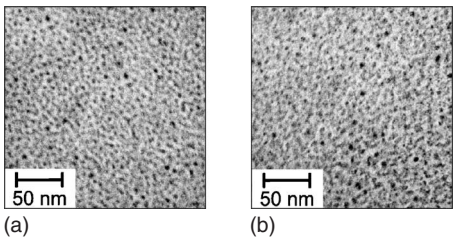

FIG. 4. Bright-field TEM images (a) for the nonirradiated OG530 sample and (b) for the same sample irradiated with the maximum peak intensity of 2.2×10^{14} W/cm^2.

fore, we could not compare the dimensions of the nanoparticles in the two regions. However, considering that in this glass the band gap is greater and hence the 780 nm multiphoton absorption is less efficient (also the color change is much lighter, see Fig. 1), we are confident that the behavior is the same as in the OG530 filter, with no significant size modification of the nanocrystals induced by femtosecond pulses.

B. Transmission electron microscopy characterization

Notwithstanding several papers that exploit the LW Raman spectra to determine the size of the nanocrystals, a recent study suggests that the mixed character of spheroidal vibrational modes of semiconductor quantum dots may lead to the appearance of a line whose spectral position is independent of the average radius of nanocrystals in the sample over a wide range of sizes.[23] To overcome this problem and also to achieve a higher accuracy in determining the size variation between the pristine material and the irradiated one, the OG530 sample was analyzed by bright-field TEM. The micrographs were taken at a magnification which allowed us to get the best compromise between cluster visibility and statistics (about 350 clusters in the analyzed region). Figure 4 reports the two TEM images corresponding to the nonirradiated region (a) and to the one irradiated with the highest peak intensity (b). The images were then treated with a commercially available software (ImageProPlus, version 3.0, MediaCibernetics L.P.) by setting a threshold value for the pixel intensity that gives sharp boundaries between clusters and background. The radius of each cluster has been determined by approximating them to spheres, with a lower limit of 1.4 nm as the smallest significant radius. The cluster radii have been plotted under the form of a histogram (Fig. 5), reporting the number of counts for all the different detected sizes. The size distribution in the nonirradiated region is not significantly different from that in the region irradiated with the maximum peak intensity of 2.2×10^{14} W/cm^2. This result confirms the conclusions drawn after the LW Raman spectra comparison, i.e., that the femtosecond laser does not change the size distribution of the nanocrystals. As a final comment regarding the nanocrystal size, it is worth noting that the average value that we retrieve from the TEM measurement is of 3 ± 1 nm, thus, in fairly good agreement with the values obtained from LW Raman spectra by Ivanda *et al.*[19] (3.9 nm), and Verma *et al.*[22] (2.2 nm).

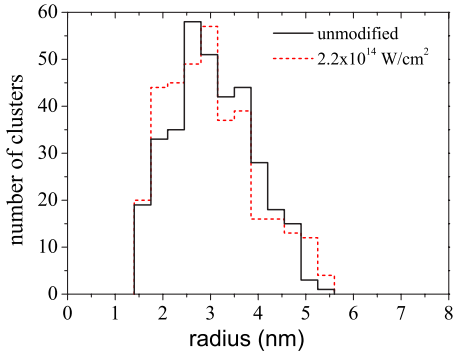

FIG. 5. (Color online) Nanocrystal radius distribution in the nonirradiated region (solid line) and in the one irradiated with the highest peak intensity (dashed line).

In conclusion, regarding composition and size of nanoparticles embedded in the glass, Raman and TEM measurements indicate that the femtosecond laser pulses do not induce any significant modification.

C. Absorption and photoluminescence spectra

The absorption spectra of the GG495 and OG530 samples, in the 450–650 nm wavelength range, are presented in Fig. 6. In both spectra, there is a redshift and a change in the curvature of the absorption edge in the irradiated zones. These effects are increasingly pronounced for higher irradiation intensities. The changes in optical density after laser irradiation with respect to the unmodified regions

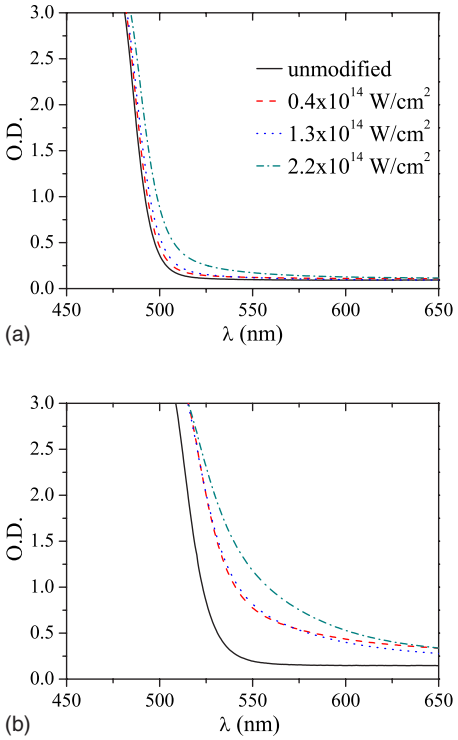

FIG. 6. (Color online) Absorption spectrum of the Schott filters before and after irradiation with different femtosecond laser peak intensities for (a) GG495 and (b) OG530.

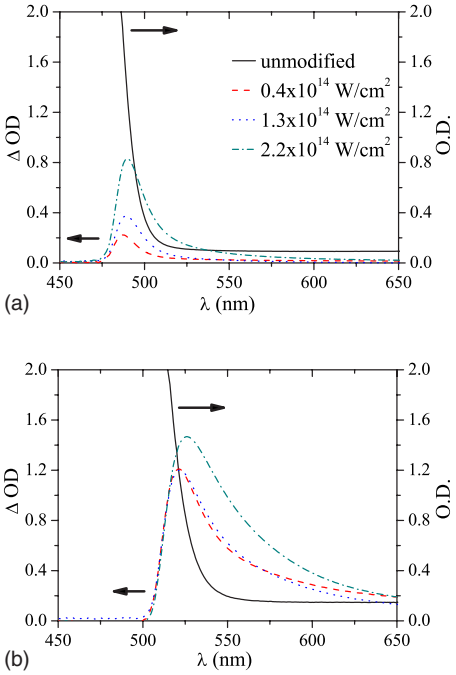

FIG. 7. (Color online) Change in the absorption spectra of the Schott filters before and after irradiation with different femtosecond laser peak intensities for (a) GG495 and (b) OG530.

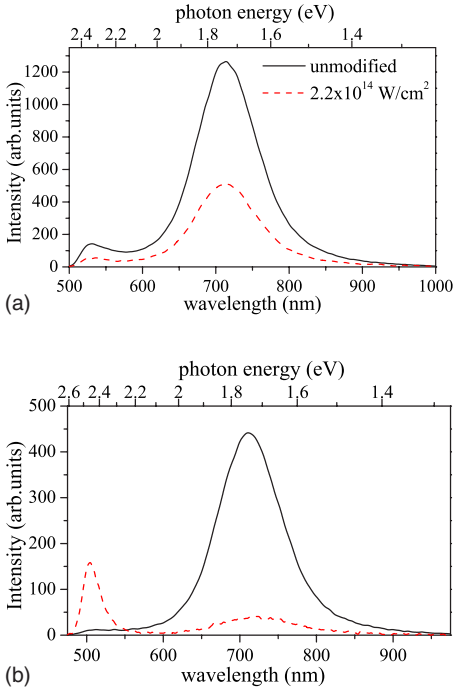

FIG. 8. (Color online) Photoluminescence in (a) OG530 and (b) GG495 excited by a laser at 488 and 457 nm, respectively. In order to have comparable signals, different excitation conditions have been used for the measurements in the unmodified and modified regions (see text). These are equivalent to multiplying the modified region signal by a factor of 1000.

are presented in Fig. 7. Here, the redshift and the smoothing of the absorption edge are more evident. The full widths at half maximum of the optical density changes for the highest irradiation intensity are 21 and 54 nm for GG495 and OG530, respectively.

In CdS_xSe_{1-x} nanocrystals embedded in glasses, the PL emission is due to direct recombination at the absorption edge and to the decay of electrons from deep trap levels to the valence band (redshifted emission).[1] These trap levels, lying far below the absorption edge, can be due to defects, vacancies, or interface states. Figure 8 presents the PL spectra for both the OG530 and the GG495 with excitation wavelengths at 488 and 457 nm, respectively. The excitation wavelengths have been chosen in order to be about 40 nm below the cutoff absorption wavelength for both glasses.

PL spectra from modified and unmodified regions of the two glasses are reported. In order to compare signals with very different intensities, PL spectra have been collected with distinct laser powers, namely, 0.1 mW for unmodified regions and 10 mW for modified ones, and different integrating times, namely, 1 s for unmodified regions and 10 s for modified ones. Assuming equal excitation conditions, this is equivalent to multiplying the modified region signal by a factor of 1000.

The PL spectra of the two glasses clearly show the contributions from both the near-band-edge emission (peak at 533 nm for the OG530 and at 500 nm for the GG495) and the deep trap emission (about 720 nm for both glasses).

For the OG530 filter, the PL spectrum in the irradiated region shows a significant decrease in intensity with respect to the original glass, but keeps almost the same shape, i.e., the relative intensities between the two PL contributions stay constant [see Fig. 8(a)]. On the other hand, as visible in Fig. 8(b), the GG495 PL spectrum varies not only in intensity but also in shape. In this case, the near-band-edge component decreases less than the deep trap one. These data indicate that in the irradiated regions, the two PL decay channels (through the deep traps and by direct recombination near the band edge) are strongly inhibited. In OG530 the two PL components keep the same relative weight, while in GG495 the deep trap PL is quenched more than the near-band-edge one.

The strong modifications both in the absorption and photoluminescence spectra after femtosecond laser irradiation can be interpreted with a single model. The nonlinear absorption of a near-infrared femtosecond pulse in a transparent material results in the creation of a free electron plasma,[6] as evidenced by the white light emitted from the focal volume during irradiation. The femtosecond laser radiation should be mainly absorbed by the nanocrystals, since their band gap is smaller than that of the glass matrix, thus allowing a less nonlinear process (two photon process with respect to a three to four photon process). Therefore, during the irradiation, a free carrier plasma is created in the nanocrystals. These conduction-band electrons gain energy from the laser field much faster than they transfer energy to the lattice.[6] After the pulse has passed, a part of the electrons decay back to the valence band through the conduction-band edge or through the deep traps, but part of these carriers have enough energy for a resonant coupling to the energy states of the glass surrounding the nanocrystals. These states, according to the energy level scheme proposed in Ref. 24, are far above the

conduction-band edge and can be accessed only by the energetic electrons. This charge displacement creates a local static electric field across the nanocrystals in the irradiated region and thus permanently modifies the optical properties of the samples.

Discussing in more detail the absorption changes, it is worth noting that the modifications of the absorption spectra for irradiated quantum dots are quite similar to those found in the presence of an external static electric field. In particular, in Ref. 25 it has been shown that for low confinement systems (nanocrystal radius $R \gg a_B$, where a_B is the excitonic Bohr radius), the change in the optical density increases its amplitude with the applied electric field but the redshift remains limited. On the other hand, in the case of more confining quantum dots (radius $R \ll a_B$) and in the presence of an external electric field, a more pronounced red shift and broadening of the optical density change have been observed.

According to the model previously discussed, the photoinduced charge transfer to the glass matrix is responsible for a static electric field across the nanocrystals; thus, the abovecited analogy is very appropriate. In the case of the GG495 filter the femtosecond laser irradiation gives a rather narrow peak in the absorption change [ΔOD in Fig. 7(a)], while for the OG530 it causes a more pronounced broadening of the absorption change [ΔOD in Fig. 7(b)]. As previously discussed, this different behavior can be understood by comparing the nanocrystal size to the corresponding exciton Bohr radius. The radii of the nanocrystals in the two glasses have been reported in the literature to be 3.8 nm for the GG495 and 3.9 nm for the OG530.[19] The corresponding Bohr radii can be calculated, as a first approximation, by linear interpolation between the known values for the CdS (a_B=2.9 nm) and CdSe (a_B=5.6 nm),[26] taking into account the CdS fraction x for the nanocrystals in the two glasses.[14] For the GG495 (x=0.853) the estimated Bohr radius is a_B=3.3 nm, while for the OG530 (x=0.698) it is a_B=3.7 nm. Even if, considering the literature values, in both cases the Bohr radius is lower than the reported particle radius, the nanocrystals in the OG530 are closer to the strong confinement regime than those in the GG495. This explains the different behavior, previously evidenced, under the photoinduced electric field. Our TEM measurement of the particle radius (3 nm) for the OG530 further supports the strong confinement regime.

Figure 7 also shows that the absorption change is directly dependent on the incident laser power density. The latter is, in fact, responsible for the number of electric charges displaced to the glass matrix and thus affects the intensity of the induced electric field across the nanocrystals. Both the peak and the broadening of the absorption change are proportional to the applied static electric field and this causes the observed behavior. Finally, it is worth noting that the absorption change amplitude in the OG530 glass is higher than in the GG495 glass. This is a consequence of the smaller band gap of the former, causing a more probable nonlinear absorption and thus a more efficient transfer of carriers to the glass matrix. This also explains why the OG530 glass shows a much more significant color change, as compared to the GG495, under the same irradiation parameters. In fact, on one hand, the higher nonlinear absorption induces a higher electric field across the nanocrystals; on the other hand, the nanocrystal dimensions, closer to the corresponding Bohr radius, favor the redshift of the absorption spectra under the photoinduced electric field.

The same charge transfer model that was introduced to explain the absorption spectra changes can also be used to provide an explanation for the strong PL quenching. The intensity reduction of PL in this kind of samples has been already observed for cw or long pulse excitation and is known as photodarkening (PD).[24,27–29] Various explanations of the PD effect have been proposed in the literature. The most convincing interpretation is analogously based on a charge transfer from the nanocrystal to the glass host matrix.[24,29] The trapping of electrons within the glass matrix in the vicinity of the semiconductor nanocrystal surface creates a repulsive Coulomb interaction that screens the trap levels, thus preventing the population of these states. As a consequence, the PL from these states is dramatically reduced. The assumption of an electric field induced by a charge transfer to the glass matrix also in the case of a femtosecond laser excitation is not only able to explain the changes in the absorption spectra but can also provide an interpretation for the PD effect. Nevertheless, the PD induced by femtosecond laser pulses presents some interesting differences with the phenomenon observed with cw or long-pulse excitation. In the latter case,[24,29] electrons in the valence band are photoexcited to the conduction band and some of them relax to trap levels at the glass-semiconductor interface. Before the electrons can recombine, light at later times in the pulse reexcites some of these trapped electrons to higher-energy surface states, from which they may migrate into the bulk of the glass. It is therefore a two-step process that is wavelength dependent since it requires a first resonant excitation. In addition, long-pulse excitation typically requires long exposure times to induce PD. Irradiation with a photon energy below the band gap is not able to induce any PD since no intermediate level is present for a two-step transfer to the glass matrix.[29] In the case of femtosecond laser excitation, it is not a two-step process but a single multiphoton process. As a consequence, the PD effect is not wavelength dependent and can happen even for photon energies far below the band gap. Moreover, in the femtosecond laser excitation the charge transfer to the glass matrix is much more efficient since the intermediate level bottleneck has been removed; in fact, excitation at high intensities to the conduction band is limited by interband absorption saturation.[29] As a consequence of the higher charge transfer yield, the femtosecond laser induced electric field across the nanocrystals is much higher and thus different effects, such as modifications of the absorption spectra and dramatic quenching of PL, become very significant with very short exposure times. As shown in Fig. 8, the deep trap PL, usually attributed to defects at the particle-glass interface, is almost completely canceled in both glasses. The near-band-edge PL is reduced proportionally only in OG530, while in GG495 it reduces less than the deep trap PL. A possible explanation for this behavior is based on the fact that the electric field, induced by the charge transfer to the glass matrix, is much

higher in OG530 than in GG495, as already mentioned several times. The repulsive Coulomb interaction that strongly shields the population of deep traps (which are typically located at the outer border of the nanocrystal) is thus able to shield also the population of the near-band-edge traps (which are uniformly distributed in the nanocrystal) more effectively in the OG530 than in the GG495.

A final important difference between PD induced by resonant excitation with cw or long laser pulses and multiphoton excitation with femtosecond laser pulses is the fact that in the latter case, the nonlinear absorption mechanism is capable of inducing PD selectively in the volume of the material without affecting the surrounding regions. This allows a complex three-dimensional (3D) structuring of the material that could find application, for example, in 3D optical memories. In fact, spatially selective modification of the photoluminescence spectrum has been proposed as a possible method for realizing 3D optical memories with densities up to 10 Tbits/cm^3, in transparent samarium doped glasses.[30,31] Here, the strong PL quenching achievable in small volume inside the nanostructured glasses with size limited by diffraction could pave the way to the development of a different generation of optical memories with the advantages of a very high signal-to-noise ratio and the availability and ease of production of the nanostructured glass substrate.

IV. CONCLUSIONS

An extensive study of the interaction between femtosecond laser pulses and CdS_xSe_{1-x} nanocrystals embedded in a borosilicate glass matrix has been presented. Absorption measurements revealed a strong absorption change close to the band gap associated with an evident color change. Raman spectra and TEM measurements evidenced that, for this pulse energy level, no modification in size and composition of the nanocrystals occurred. Photoluminescence measurements showed that a strong signal quenching is present in the irradiated region. All these results have been interpreted by a simple model based on nanocrystal ionization due to nonlinear absorption of the laser pulse and charge transfer to the glass matrix.

ACKNOWLEDGMENT

We wish to acknowledge partial financial support by Fondazione Politecnico di Milano (research program "Advanced materials and devices for Photonics").

*roberto.osellame@polimi.it

[1] U. Woggon, *Optical Properties of Semiconductor Quantum Dots* (Springer-Verlag, Berlin, 1997).
[2] These filters are commercially available, for example, from Corning Glass Industries, Schott Optical Glasses, and Hoya.
[3] G. Bret and F. Gires, Appl. Phys. Lett. **4**, 175 (1964).
[4] L. H. Acioli, A. S. L. Gomes, J. R. Rios Leite, and C. B. De Araujo, IEEE J. Quantum Electron. **26**, 1277 (1990).
[5] J. Magyar, C. Aita, M. Gajdardziska-Josifovska, A. Sklyarov, K. Mikhaylichenko, and V. V. Yakovlev, Appl. Phys. A: Mater. Sci. Process. **77**, 285 (2003).
[6] B. C. Stuart, M. D. Feit, A. M. Rubenchik, B. W. Shore, and M. D. Perry, Phys. Rev. Lett. **74**, 2248 (1995).
[7] R. Osellame, N. Chiodo, G. Della Valle, S. Taccheo, R. Ramponi, G. Cerullo, A. Killi, U. Morgner, M. Lederer, and D. Kopf, Opt. Lett. **29**, 1900 (2004).
[8] M. Kaempfe, T. Rainer, K.-J. Berg, G. Seifert, and H. Graener, Appl. Phys. Lett. **74**, 1200 (1999).
[9] S. Link, C. Burda, B. Nikoobakht, and M. A. El-Sayed, J. Phys. Chem. B **104**, 6152 (2000).
[10] G. Seifert, M. Kaempfe, K.-J. Berg, and H. Graener, Appl. Phys. B: Lasers Opt. **73**, 355 (2001).
[11] D. Mangaiyarkarsai, K. Kamada, N. Saito, S. Ichikawa, T. Akai, K. Kadono, and T. Yazawa, J. Non-Cryst. Solids **351**, 3156 (2005).
[12] V. Klimov, P. H. Bolivar, and H. Kurz, Phys. Rev. B **53**, 1463 (1996).
[13] C. Momma, S. Nolte, B. N. Chichkov, F. v. Alvensleben, and A. Tuennermann, Appl. Surf. Sci. **109/110**, 15 (1997).
[14] T. Bischof, M. Ivanda, G. Lermann, A. Materny, W. Kiefer, and J. Kalus, J. Raman Spectrosc. **27**, 297 (1996).
[15] M. Ivanda, T. Bischof, G. Lermann, A. Materny, and W. Kiefer, J. Appl. Phys. **82**, 3116 (1997).
[16] A. Tu and P. D. Persans, Appl. Phys. Lett. **58**, 1506 (1991).
[17] A. V. Gomonnai, Y. M. Azhniuk, V. O. Yukhymchuk, M. Kranjcec, and V. V. Lopushansky, Phys. Status Solidi B **239**, 490 (2003).
[18] Y. M. Azhniuk, A. G. Milekhin, A. V. Gomonnai, V. V. Lopushansky, V. O. Yukhymchuk, S. Schulze, E. I. Zenkevich, and D. R. T. Zahn, J. Phys.: Condens. Matter **16**, 9069 (2004).
[19] M. Ivanda, K. Babocsi, C. Dem, M. Schmitt, M. Montagna, and W. Kiefer, Phys. Rev. B **67**, 235329 (2003).
[20] E. Duval, Phys. Rev. B **46**, 5795 (1992).
[21] G. Irmer, J. Monecke, P. Verma, G. Goerigk, and M. Herms, J. Appl. Phys. **88**, 1873 (2000).
[22] P. Verma, W. Cordts, G. Irmer, and J. Monecke, Phys. Rev. B **60**, 5778 (1999).
[23] S. V. Gupalov and I. A. Merkulov, JETP Lett. **72**, 49 (2000).
[24] T. Bischof, G. Lermann, B. Schreder, A. Materny, W. Kiefer, and M. Ivanda, J. Opt. Soc. Am. B **14**, 3334 (1997).
[25] A. I. Ekimov, Al. L. Efros, T. V. Shubina, and A. P. Skvortsov, J. Lumin. **46**, 97 (1990).
[26] W. Martienssen and H. Warlimont, *Springer Handbook of Condensed Matter and Materials Data* (Springer, Berlin, 2005).
[27] P. Roussignol, D. Ricard, J. Lukasik, and C. Flytzanis, J. Opt. Soc. Am. B **4**, 5 (1987).
[28] M. Tomita and M. Matsuoka, J. Opt. Soc. Am. B **7**, 1198 (1990).
[29] J. Malhotra, D. J. Hagan, and B. G. Matsuoka, J. Opt. Soc. Am. B **8**, 1531 (1991).
[30] K. Miura, J. Qiu, S. Fujiwara, S. Sakaguchi, and K. Hirao, Appl. Phys. Lett. **80**, 2263 (2002).
[31] J. Lim, M. Lee, and E. Kim, Appl. Phys. Lett. **86**, 191105 (2005).